

1 **Drivers of Australian dust: a case study of frontal winds and dust dynamics in the lower**
2 **Lake Eyre Basin**

3
4 M.C. Baddock^{1*}, K. Parsons², C.L. Strong³, J.F. Leys⁴ and G.H. McTainsh²

5
6 ¹Department of Geography, Loughborough University, Loughborough, Leicestershire UK
7 LE11 3TU

8
9 ²Griffith School of Environment, Griffith University, Brisbane, Queensland, Australia 4111

10
11 ³Fenner School of Environment and Society, Australian National University, Canberra,
12 Australian Capital Territory, Australia 0200

13
14 ⁴Office of Environment and Heritage, Science Division, Gunnedah, New South Wales,
15 Australia 2380

16
17 *Corresponding author

18 Tel: +44 (0)1509 222798

19 Fax: +44 (0)1509 223930

20 Email: m.c.baddock@lboro.ac.uk

21
22 **ABSTRACT**

23 The roles of pre-frontal, frontal and post-frontal winds as the primary wind systems for dust
24 entrainment and transport in Australia are well established. While the relevance of each
25 system has been observed across different wind erosion events in central Australia, the
26 entrainment of dust by all three winds during the passage of an individual front has not been
27 demonstrated until now. Synoptic information, satellite aerosol and imagery, meteorological
28 and dust concentration data are presented for a single case study erosion event in the lower
29 Lake Eyre Basin. This event demonstrates variable dust transport in three different directions
30 from one of the southern Hemisphere's most significant source regions, and the changing
31 nature of the active dust pathways during the passage of a frontal system. While only a single
32 dust event is considered, the findings show the complexity of mineral aerosol emission and
33 transport patterns even within an individual dust outbreak. For the lower Lake Eyre Basin,
34 this appreciation of pathway behaviour is significant for better understanding the role of

35 aeolian inputs from the dominant Australian source to surrounding marine systems. In a
36 wider context, the findings exhibit the detailed insights into major dust source dynamics that
37 can be obtained from high resolution spatial and particularly temporal data, as used in
38 combination. This work highlights the importance of adequately resolved data for the
39 accurate determination of dust entrainment and transport patterns of major dust sources.

40

41 1. INTRODUCTION

42 Australia is a principal contributor to mineral aerosol in the southern hemisphere, with the
43 major atmospheric driver of dust emission from the continent being the westerly passage of
44 frontal systems across its lower half (McTainsh and Leys, 1993; Leslie and Speer 2006). In
45 particular, the operation of three different ‘wind systems’ in producing dust over Australia is
46 clearly recognised (e.g., Sprigg 1982, Strong et al. 2011). Pre-frontal northerly winds which
47 occur ahead of a front are frequently strong enough to raise dust in advance of the front as it
48 moves across the continent. The arrival of the leading edge of the front itself is typically
49 associated with well-developed westerly winds which have the potential to entrain especially
50 large quantities of dust. These westerlies can raise dust along an extended line aligned
51 roughly north-south, and are characterised by rolling dust storms with snouts often hundreds
52 of kilometres in length (Leslie and Speer 2006). As such, this mechanism tends to produce
53 Australia’s largest dust storms (McTainsh et al., 2005, Leys et al., 2011). Finally, the
54 southerly winds of a post-frontal nature can also entrain dust if they are strong enough to
55 exceed the threshold for suspension of surface sediments.

56

57 The geomorphic role of these three wind systems in the entrainment and off-continent
58 transport of dust is well appreciated in Australia (e.g., Bowler, 1976; Sprigg, 1982,
59 McTainsh, 1989) and the three systems are associated with a classic wind-dust pattern
60 associated with fronts (Figure 1). Bowler (1976) was first to propose there were two major
61 dust paths operating in Australia during the Quaternary; the South East Dust Path and the
62 North West Dust Path. He noted that the semi-circular, continental scale pattern of linear
63 dunes in central Australia must also reflect the predominant dust transporting winds. Sprigg
64 (1982) concluded from measurements in the Strzelecki and Simpson dunefields that three
65 wind systems were responsible for entraining and transporting dust within these two dust
66 paths. Subsequent wind erosion mapping (summarised by McTainsh, 1989), studies of
67 individual dust storm events (e.g. Raupach et al., 1994; McTainsh et al., 2005) and air
68 trajectory modelling (McGowan and Clark, 2008) have provided clear evidence that the three

69 wind system model associated with cold fronts is the main mechanism for dust entrainment
70 and transport in Australia.

71

72 << Figure 1 >>

73

74 More recently, Strong et al. (2011) investigated the occurrence of these three wind systems in
75 further detail, finding that over half the total dust days in the Lake Eyre Basin (2005-2006)
76 were generated by frontal activity as a whole (i.e. pre-frontal northerly, frontal westerly and
77 post-frontal southerly winds). Subtropical cold fronts are the most significant meteorological
78 feature affecting central Australia (Beringer and Tapper, 2000) and their structure, behaviour
79 and impact on surface energy exchanges were investigated in a series of field experiments
80 (Central Australian Fronts Experiment) in 1991 (CAFE91) (Smith *et al.*, 1995) and 1996
81 (CAFE96) (Reeder et al., 2000; Beringer and Taper, 2000). Fronts were typically found to
82 produce strong pressure gradients across the front lines capable of producing winds of high
83 speeds (Smith *et al.*, 1995). Pre-frontal troughs and heat troughs were also identified as
84 producing wind shifts similar to that of frontal systems, and are therefore also associated with
85 the entrainment of dust. Reeder and Smith (1992) describe the replacement of hot, dry
86 northerly winds with cooler southwesterly winds during spring and summer cold front
87 episodes, and winds shifting anticlockwise with the passage of the front (Reeder et al., 2000).

88

89 This paper uses synoptic information, satellite imagery, wind speed/direction and dust
90 concentration data from a single, large scale wind erosion event to demonstrate the operation
91 of the principal wind systems for dust emission and transport in Australia. The case study
92 event is notable as it reveals entrainment of dust by the three front-related wind systems, and
93 that time-dependent shifts in dust transport pathway, can occur through the passage of a
94 single front over the continent.

95

96 2. BACKGROUND

97 The dominant dust source region of Australia and a prominent mineral aerosol source in the
98 southern hemisphere is the arid Lake Eyre Basin (LEB) (Prospero et al., 2002). Like most
99 major dust source regions, different land surface types within the LEB have variable potential
100 to emit dust as controlled by sediment supply and surface erodibility (Bullard et al., 2008;
101 Bullard et al., 2011). Internally draining fluvial systems are important in transporting fine
102 sediments to the lower reaches of major ephemeral rivers such as Cooper Creek and the

103 Diamantina River, and terminal, occasionally inundated lakes such as Lake Eyre North
104 (LEN). When dry, these river floodplains and lake beds often act as sources of dust (Bullard
105 and McTainsh, 2003; Prospero et al., 2002; Bullard et al., 2008). Flooding of LEN in early
106 2009, produced a quiescence of dust activity which was prolonged by the existence of moist,
107 stabilised lake surface sediments. By the austral Spring of 2013, however, LEN had dried and
108 become erodible again.

109

110 A wind erosion event indicating the reversion of LEN to an active dust source occurred in
111 mid October 2013. This frontally-driven dust outbreak was noteworthy because the
112 occurrence of its three stages coincided with the timing of (cloud free) satellite overpasses,
113 enabling its full development to be captured by moderate resolution imagery. The
114 coincidence of the imagery and the event illustrates the temporal evolution through space of
115 the different wind systems and their associated dust activity.

116

117 3. METHODS

118 To characterise the dust event, mean sea level pressure charts were obtained from the
119 Australian Bureau of Meteorology (ABM). High frequency dust concentration data for the
120 region was available from equipment operated by an Australian dust monitoring network
121 known as DustWatch (<http://www.environment.nsw.gov.au/dustwatch/>) (Leys et al., 2008).
122 Three (Moolawatana, Birdsville and Tibooburra) of the 42 instrumented DustWatch locations
123 were used in this study (Figure 2).

124

125 <<Figure 2>>

126

127 Each site consists of an aerosol monitor (DustTrak® model 8520 inside the manufacturer's
128 weatherproof environmental enclosure) that measures the atmospheric aerosol concentration
129 of particulate matter <10 µm diameter (PM₁₀). These instruments sample every 15 minutes,
130 increasing to one minute frequency when PM₁₀ concentration exceeds 25 µg/m³. Factory
131 calibration is undertaken annually by the Australian distributor, adjusted to respirable mass
132 standard ISO 12103-1 A1 Test Dust (Arizona Dust). Calibration for a particular source
133 material is not warranted as the sampling network covers 42 sites across southern Australia
134 with multiple dust source types. Instruments are calibrated on site each month to have a zero
135 (clean air) reading of ±0.003 mg/m³. Inlets are cleaned and water bottles are also emptied. To
136 overcome instrument drift, every 15 minutes a zero reading is taken through the

137 manufacturer's 'zero filter' and stored in the database. This value is then subtracted from all
138 ambient readings until the next zero filter reading is taken. All data are stored and publically
139 accessible via the Community DustWatch information interface (CoDii).

140

141 Data are remotely polled by CoDii on a daily basis at 1000 Australian Eastern Daylight Time
142 (EDT), and the calculated hourly averaged aerosol concentrations are quality controlled.

143 Meteorological data from the nearest ABM station is also downloaded and used in
144 conjunction with NASA Moderate Resolution Imaging Spectrometer (MODIS) Rapid
145 Response data to partition the hourly reading into dust, smoke or fog using the following
146 rules. 1) Dust values $<0.010 \mu\text{g}/\text{m}^3$ are disregarded, 2) data is flagged as fog if humidity is
147 $>80\%$ and wind speed is low ($< 20\text{km}/\text{h}$) and/or the coupled meteorological observation
148 reported fog at that time, 3) data is flagged as smoke if windspeeds $<30 \text{ km}/\text{h}$ for the 3 hours
149 preceding and subsequent to the value, or windspeeds $<10 \text{ km}/\text{h}$ and fires or smoke were
150 detected within the area (ascertained from global fire mapping by MODIS FIRMS), 4) a
151 malfunction if dust values are <0 , are extremely erratic or the DustTrak displays an error
152 message. Only hourly averaged values successfully flagged as dust are used in this study and
153 more information is available from the CoDii manual

154 (<http://www.environment.nsw.gov.au/resources/dustwatch/CoDiiManual.pdf>).

155

156 Hourly wind speed and direction at 10 m height were derived from the ABM station
157 observing closest to each DustWatch site. At Birdsville and Tibooburra, the DustWatch and
158 ABM stations are within 1 km of each other, but at Moolawatana, a remote cattle station
159 operating DustWatch equipment, meteorological data from the ABM station at Marree (170
160 km to the west) were used for this study (Figure 2).

161

162 Data from the MODIS instrument mounted on both the Terra and Aqua platforms were used
163 to observe the dust event. 'True colour' scenes produced by the NASA LANCE Rapid
164 Response system for the 10th October 2013 were obtained, as well as the level 1 MODIS data
165 to produce a simple bi-spectral 'split window' enhancement of the dust in scenes. Based on
166 the contrasting thermal properties of elevated dust and the land surface, the brightness
167 temperature difference (BTD) resulting from subtraction of MODIS bands 31 and 32 is
168 effective in highlighting the appearance of dust (Ackerman, 1997; Baddock et al., 2009). The
169 Deep Blue level 2 MODIS aerosol product (10 km spatial resolution at nadir) was also
170 obtained for the relevant Aqua overpass (0525 UTC, 10th October). The Deep Blue product is

171 derived from an algorithm using multiple MODIS band data to provide an estimation of
172 aerosol optical depth (AOD) designed for better performance over bright desert surfaces (Hsu
173 et al., 2004). It has been used in investigations of dust source dynamics (e.g., Ginoux et al.,
174 2010; Baddock et al., 2009; Ginoux et al., 2012) and its full development and details are
175 described by Hsu et al. (2004). The latest Collection 6 MYD04 data are used here (Hsu et al.,
176 2013).

177

178 4. RESULTS AND DISCUSSION

179 *4.1 Synoptic development*

180 On 9th October 2013 at 1100 EDT, a high pressure system was positioned over the east coast
181 of Australia, generating pre-frontal northerly winds over southern and central Queensland,
182 New South Wales and South Australia. A trough system associated with an embedded area of
183 low pressure extended northwesterly from the Great Australian Bight, with a cold front
184 located to the south (Figure 3a). The high pressure cell and trough contracted eastward by
185 2300 EDT, with the trough and low pressure cell becoming situated over central South
186 Australia. At this time, the trough system linked with the cold front to the south, and formed
187 an extension trough (Figure 3b).

188

189 >> Figure 3 <<

190

191 By 1700 EDT on 10th October, a strong pressure gradient had developed between the low
192 pressure trough (now over mid New South Wales and northeastern South Australia) and the
193 high pressure cell (Figure 3c). This pressure gradient generated strong post-frontal southerly
194 winds over most of southeastern New South Wales and South Australia. Abrupt changes in
195 wind direction were observed at lower LEB observation stations around 1900-2000 EDT as
196 the front passed through the region at this time (see section 4.3). Winds demonstrated rapid
197 backing in an anticlockwise direction from predominantly NNW, through W, to SSW. The
198 central pressure of the embedded low pressure cell was 999 hPa by now, with another low
199 pressure cell evident at the southern end of the trough line (994 hPa central pressure) (Figure
200 3c). By 2300 EDT, the trough had continued to the northeast, with the following high
201 pressure cell positioned at the Western Australia-South Australia border, producing post-
202 frontal southerly winds throughout the lower LEB (Figure 3d).

203

204 *4.2 Dust event imagery*

205 The broad spatial pattern of dust activity is revealed by MODIS imagery from the local
206 morning and afternoon overpasses of the Terra and Aqua satellites respectively (Figure 4).

207

208 << Figure 4 >>

209

210 During the morning of 10th October 2013, the 1205 EDT MODIS image showed large dust
211 plumes emanating from the northern part of LEN and moving in a southeasterly direction
212 (Figure 4a). This northern part of LEN and the major ephemeral entry channel into the lake
213 from the north, called the Warburton Groove, represented erodible surfaces covered by fine
214 sediments that had been deposited by the flooding events of 2009 onwards. The presence of
215 these deposits is evident from the contrast of the darker surface of sediment in the north with
216 the white, salt-crusted surface in the southern part of the lake (Figure 4a).

217

218 The 1625 EDT afternoon scene reveals LEN was still actively emitting dust some four hours
219 after the morning image, but by 1625 EDT the heading of its dust plumes had shifted to the
220 northeast (Box A, Figure 4b,c). Furthermore, a strongly linear ‘wall’ of dust can be seen
221 extended diagonally from the southeast to the northwest across the scene, appearing
222 particularly clearly in the BTM enhancement (Box B, Figure 4b,c). This dust wall evidently
223 developed in the time since the 1205 Terra image. Another notable feature is the emission of
224 dust at 1625 EDT from Lake Cadibarrawirracanna, a small dry lake west of LEN. At 1625
225 EDT dust blew from this source in a NNW direction (Box C, Figure 4b), and is also apparent
226 in the Deep Blue AOD retrieval for that time (Figure 4d). Elevated AOD was identified
227 downwind of LEN, with the Deep Blue retrieval also picking out the densest parts of the wall
228 of dust.

229

230 *4.3 Wind speeds, direction and measured dust concentration*

231 The timing and spatial development of the dust observed in the imagery can be linked to the
232 recorded wind speeds, directions and dust concentration at the three DustWatch sites plus
233 Marree meteorological station (Figure 2). The dust source areas and plume pathways vary in
234 accordance with changes in the three wind systems. During the course of the event, as the
235 front passed across the lower LEB, the wind shifted from north through west, to south and
236 southwest.

237

238 On the morning of 10th October, the pre-frontal synoptic situation produced north to
239 northeasterly winds across central Australia (Figure 3a), which were recorded at all three
240 DustWatch stations (Figure 5). Through the morning at Moolawatana, wind strength
241 intensified from around 3 m/s (0800 EDT) to peak at 11 m/s (1000 EDT) and wind direction
242 shifted from northerly through west-northwest to westerly. Figure 4b indicates light coloured
243 dust transported in a southeast direction under these pre-frontal winds at 1205 EDT, and the
244 dust concentration at Moolawatana (320 km SE of LEN) shows the arrival of the dust on
245 these winds at 1500 EDT, three hours later (Figure 5a).

246

247 <<Figure 5>>

248

249 While the wind direction at the time of peak dust concentration at Moolawatana had become
250 south-southwesterly, the plume direction evident in Figure 4b, and observations at Marree of
251 northwesterly flow from 0900-1100 EDT indicate that dust entrainment and transport to
252 Moolawatana was the result of pre-frontal winds (Figure 5a). The seeming disparity between
253 the wind direction at the time of dust arrival is due to the enforced use of meteorological data
254 from Marree, located 170 km west of Moolawatana. When the wind direction switched to be
255 consistently from the southwest, Moolawatana was no longer downwind of the LEN source,
256 and this led to the rapid diminishing of dust concentration there by 1700 EDT. The distinctive
257 shift in wind direction, from the west to the southwest, marks the passage of the front. While
258 the speeds of post-frontal southerlies continued to exceed 14 m/s from 1700 EDT onwards,
259 these did not generate significant dust loads at Moolawatana because there was no active dust
260 source to the south (Figure 4a).

261

262 At Birdsville, when the pre-frontal northerly winds reached their peak at 1000 EDT, dust
263 concentration showed only a small coincident increase ($40 \mu\text{g}/\text{m}^3$) (Figure 5b). The limited
264 dust response at this time suggests that only local source surfaces to the north of Birdsville
265 were emitting during these winds. While not evident in the imagery, these sources were most
266 likely to be entrainment from the highly erodible Diamantina floodplain (Channel Country)
267 that Birdsville is sited on (seen to north of Birdsville in Figure 4a) (McTainsh et al., 1999).
268 The largest dust concentration at Birdsville ($800 \mu\text{g}/\text{m}^3$) was related to westerly winds at the
269 leading edge of the front. Elevated concentrations associated with dust transport were first
270 detected there at 2000 EDT. This rise marked the arrival in Birdsville of the dust wall seen
271 just north of LEN in the 1625 EDT imagery, with the dust having been entrained from LEN

272 and throughout the lower Simpson Desert (Figure 4b), and the Birdsville concentration
273 maximum occurring at 2100 EDT. A third (minor) increase in dust concentration ($60 \mu\text{g}/\text{m}^3$)
274 occurred between 0800-0900 EDT on 11th October. This dust was associated with an
275 increase in post-frontal southerly winds to around 10 m/s (Figure 5b), possibly sourced again
276 from the Diamantina River floodplain, this time to the south of Birdsville.

277

278 The peak dust concentration observed at Tibooburra (Figure 5c) was lower than the other two
279 stations. The concentration profile showed little increase during the afternoon of the 10th
280 October despite high pre-frontal northerly wind speeds. The arrival of the front was marked
281 by a change in wind direction as flow came from the west, resulting in the timing of
282 maximum dust concentration at 2000 EDT ($40 \mu\text{g}/\text{m}^3$). This modest peak concentration was
283 one twentieth of that for Birdsville, reflecting the greater distance of Tibooburra from the
284 active LEN source (Figure 2), and the lower local erodibility of Tibooburra compared with
285 the alluvial and dunefield surfaces local to Birdsville. In October 2013, the Tibooburra area
286 retained a relatively low erodibility due to the presence of vegetation cover induced by the
287 wet period responsible for the 2010 LEB flooding. As local surface erodibility was low, the
288 strongest likelihood is that the dust detected at Tibooburra was distantly sourced from the
289 active LEN emission. Following the passage of the front, wind speeds began to decline over
290 time and moved to southerlies without producing any dust response at Tibooburra.

291

292 5. SUMMARY

293 Synoptic analyses of central Australia, the availability of appropriately timed satellite
294 imagery, plus synergistic surface meteorological and dust concentration measurements have
295 provided an opportunity to examine, for the first time in a single event, the dynamics of the
296 three main wind systems responsible for dust entrainment in the lower Lake Eyre Basin.
297 While only a single case study is presented, here we show that during the passage of an
298 individual front, dust entrainment can occur as a result of all three wind systems. This has the
299 potential to produce dust transport in three directions, to the south east (with pre-frontal
300 northerlies), the north east (with frontal south westerlies) and to the north west (with post-
301 frontal southerlies), even in one dust outbreak. This case study illustrates the complex nature
302 of the wind systems that drive dust emission and transport in the Lake Eyre Basin, one of the
303 southern hemisphere's most significant dust sources. While the operation of the different
304 wind systems has important implications for the accurate mapping of dust activity within this
305 region, a larger study encompassing multiple events is required for a truly better developed

306 understanding of the transport pathways. An important impetus for this research comes from
307 efforts to tackle large scale interactions at the heart of Earth Systems Science, as a more
308 accurate appreciation of dust activity can help constrain the timing and location of
309 transported dust in relation to specific marine responses (e.g., possible phytoplankton blooms
310 from aeolian fertilisation).

311

312 Furthermore, the findings from this single case study serve to illustrate the type of data
313 required for improved understanding of the erosional and transport role of wind systems in
314 other dust bearing regions. Considerably higher degrees of detail can be added to our
315 understanding of dust processes at a large basin scale with a range of data resolved
316 sufficiently to capture the effects of changeable wind speed and direction, even during the
317 passage of individual dust-producing weather systems.

318

319 ACKNOWLEDGEMENTS

320 This research was possible due to contributions from the New South Wales Office of
321 Environment and Heritage (OEH) DustWatch Team (Stephan Heidenreich, Michael Case,
322 Joanne Brady) and the DustWatch volunteers at Birdsville (Senior Constable Neale
323 McShane), Moolawatana Station (Audrey Sheehan) and Tibooburra (Shane McDermott) - we
324 are extremely grateful for their excellent efforts. The Community DustWatch project was
325 funded by the NSW OEH and Caring for Our Country funding (Project A0000007342g) from
326 the Australian Government. The MODIS aerosol data used in this study were acquired as part
327 of the NASA's Earth-Sun System Division and archived and distributed by the MODIS
328 Adaptive Processing System (MODAPS), and we acknowledge use of Rapid Response
329 imagery from the Land, Atmosphere Near real-time Capability for EOS (LANCE) system
330 operated by the NASA/GSFC/Earth Science Data and Information System (ESDIS) with
331 funding provided by NASA/HQ. We also thank the input of three anonymous reviewers and
332 editorial comments for improving the manuscript.

333

334

335 REFERENCES

336 Ackerman SA. 1997. Remote sensing aerosols using satellite infrared observations. *Journal*
337 *of Geophysical Research* **102**: 17069-17080.

338

339 Baddock MC, Bullard JE, Bryant RG. 2009. Dust source identification using MODIS: A
340 comparison of techniques applied to the Lake Eyre Basin, Australia. *Remote Sensing of*
341 *Environment* **113**: 1511-1528.

342

343 Beringer J, Tapper NJ. 2000. The influence of subtropical cold fronts on the surface energy
344 balance of a semi-arid site. *Journal of Arid Environments* **44**: 437-450.

345

346 Bowler JM. 1976. Aridity in Australia - age, origins and expression in aeolian landforms and
347 sediments. *Earth-Science Reviews* **12**: 279-310.

348

349 Bullard JE, McTainsh GH. 2003. Aeolian-fluvial interactions in dryland environments:
350 examples, concepts and Australia case study. *Progress in Physical Geography* **27**: 471-501.

351

352 Bullard J, Baddock M, McTainsh G, Leys J. 2008. Sub-basin scale dust source
353 geomorphology detected using MODIS. *Geophysical Research Letters* **35**: L15404.

354

355 Bullard JE, Harrison SP, Baddock MC, Drake N, Gill TE, McTainsh G, Sun Y. 2011.
356 Preferential dust sources: a geomorphological classification designed for use in global dust-
357 cycle models. *Journal of Geophysical Research – Earth Surfaces*, 116, F04034.

358

359 Ginoux P, Garbuzov D, Hsu NC. 2010. Identification of anthropogenic and natural dust
360 sources using Moderate Resolution Imaging Spectroradiometer (MODIS) Deep Blue level 2
361 data. *Journal of Geophysical Research* **115**: D05204.

362

363 Ginoux P, Prospero JM, Gill TE, Hsu NC, Zhao M. 2012. Global-scale attribution of
364 anthropogenic and natural dust sources and their emission rates based on MODIS Deep Blue
365 aerosol products. *Reviews of Geophysics* **50**: RG3005.

366

367 Hsu NC, Tsay S-C, King M, Herman JR. 2004. Aerosol properties over bright-reflecting
368 source regions. *IEEE Transactions on Geoscience and Remote Sensing* **42**: 557– 569.

369

370 Hsu NC, Jeong M-J, Bettenhausen C, Sayer AM, Hansell R, Seftor CS, Huang J, Tsay S-C.
371 2013. Enhanced Deep Blue aerosol retrieval algorithm: The second generation. *Journal of*
372 *Geophysical Research-Atmospheres* **118**: 9296–9315. doi:10.1002/jgrd.50712

373

374 Leslie LM, Speer MS. 2006. Modelling dust transport over central eastern Australia.
375 *Meteorological Applications* **13**: 141-167.

376

377 Leys J, McTainsh G, Strong C, Heidenreich S, Biesaga K. 2008. DustWatch: using
378 community networks to improve wind erosion monitoring in Australia. *Earth Surface*
379 *Processes and Landforms* **33**: 1912-1926.

380

381 Leys JF, Heidenreich SK, Strong CL, McTainsh GH, Quigley S. 2011. PM10 concentrations
382 and mass transport during “Red Dawn” – Sydney, 23 September 2009. *Aeolian Research* **3**:
383 327-342.

384

385 McGowan H, Clark A. 2008. Identification of dust transport pathways from Lake Eyre,
386 Australia using Hysplit. *Atmospheric Environment* **42**: 6915-6925.

387

388 McTainsh GH. 1989. Quaternary aeolian dust processes and sediments in the Australian
389 region. *Quaternary Science Reviews* **8**: 235-253.

390

391 McTainsh GH, Leys JF, Nickling WG. 1999. Wind erodibility of arid lands in the Channel
392 Country of western Queensland, Australia. *Zeitschrift für Geomorphologie* **116**: 113-130.

393

394 McTainsh GH, Chan Y, McGowan H, Leys JF, Tews EK. 2005. The 23rd October 2002 dust
395 storm in eastern Australia: characteristics and meteorological conditions. *Atmospheric*
396 *Environment* **39**: 1227-1236.

397

398 Prospero JM, Ginoux P, Torres O, Nicholson SE, Gill TE. 2002. Environmental
399 characterization of global sources of atmospheric soil dust identified with the Nimbus 7 Total
400 Ozone Mapping Spectrometer (TOMS) absorbing aerosol product. *Reviews of Geophysics* **40**:
401 art. no. 1002.

402

403 Raupach MR, McTainsh GH, Leys JF. 1994. Estimates of dust mass in recent major dust
404 storms. *Australian Journal of Soil and Water Conservation* **7**: 20–24.

405

406 Reeder MJ, Smith RK, Deslandes R, Tapper NJ, Mills GA. 2000. Subtropical fronts observed
407 during the 1996 Central Australian Fronts Experiment. *Australian Meteorological Magazine*
408 **49**: 181-200.

409

410 Reeder MJ, Smith RK. 1992. Australian spring and summer cold fronts. *Australian*
411 *Meteorological Magazine* **41**: 101-124.

412

413 Sprigg RC. 1982. Some stratigraphic consequences of fluctuating Quaternary sea levels and
414 related wind regimes in southern and central Australia. In: *Quaternary dust mantles, China,*
415 *New Zealand and Australia*. Wasson RJ. ed. pp. 211-240. Australian National University:
416 Canberra.

417

418 Strong CL, Parsons K, McTainsh GH, Sheehan A. 2011. Dust transporting wind systems in
419 the lower Lake Eyre Basin, Australia: A preliminary study. *Aeolian Research* **2**: 205-214.

420

421 Smith RK, Reeder MJ, Tapper NJ, Christie DR. 1995. Central Australian cold fronts.
422 *Monthly Weather Review* **123**: 16–38.

423

424

425

426

427

428

429

430

431

432

433

434

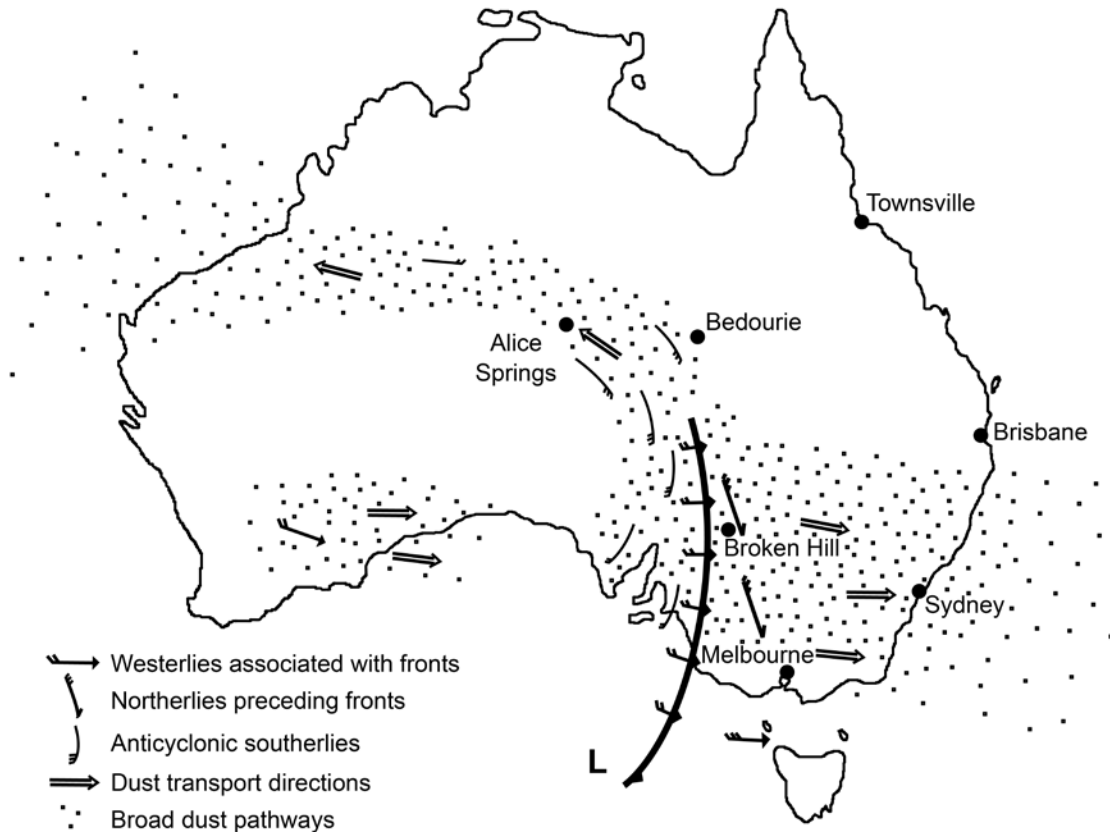
435

436

437

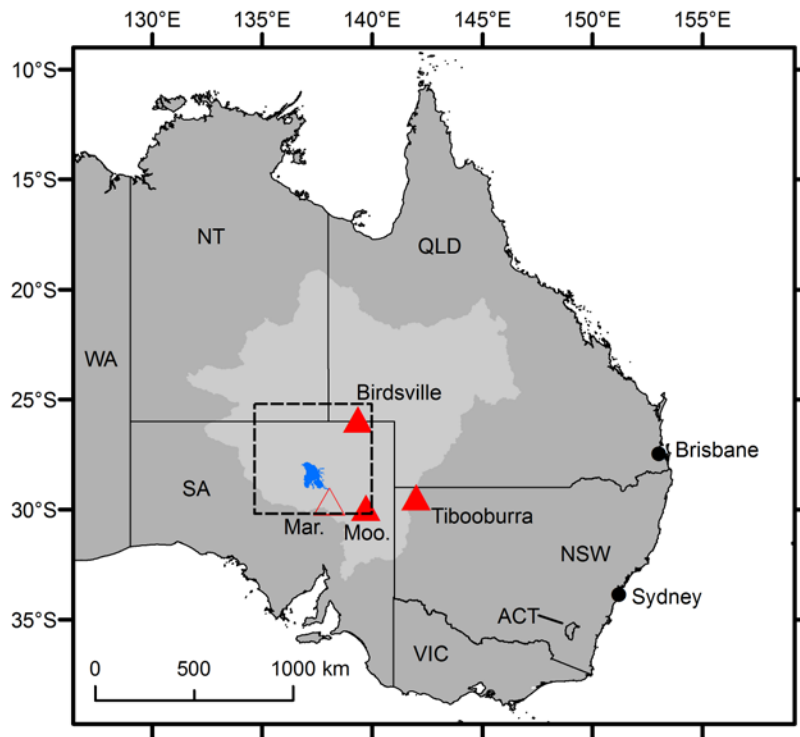
438

439



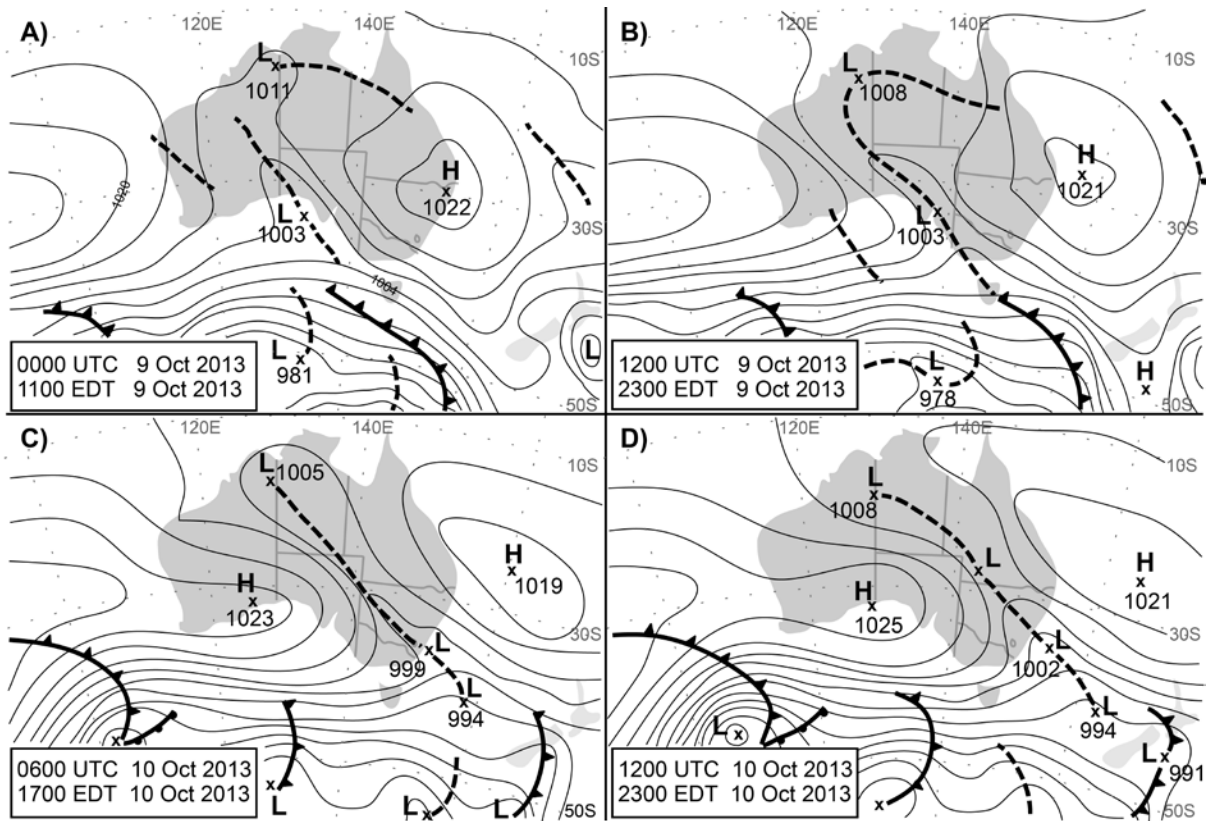
440

441 Figure 1: Sprigg's model of dust transporting winds in Australia (after Sprigg, 1982).



442

443 Figure 2: Regional context showing the Lake Eyre Basin (light grey), Lake Eyre North (blue)
 444 and locations of both dust and meteorology (solid triangle), and meteorology only (open
 445 triangle) observations. Abbreviations: Mar. (Marree), Moo. (Moolawatana). Dashed square is
 446 region covered by imagery panels in Figure 4.



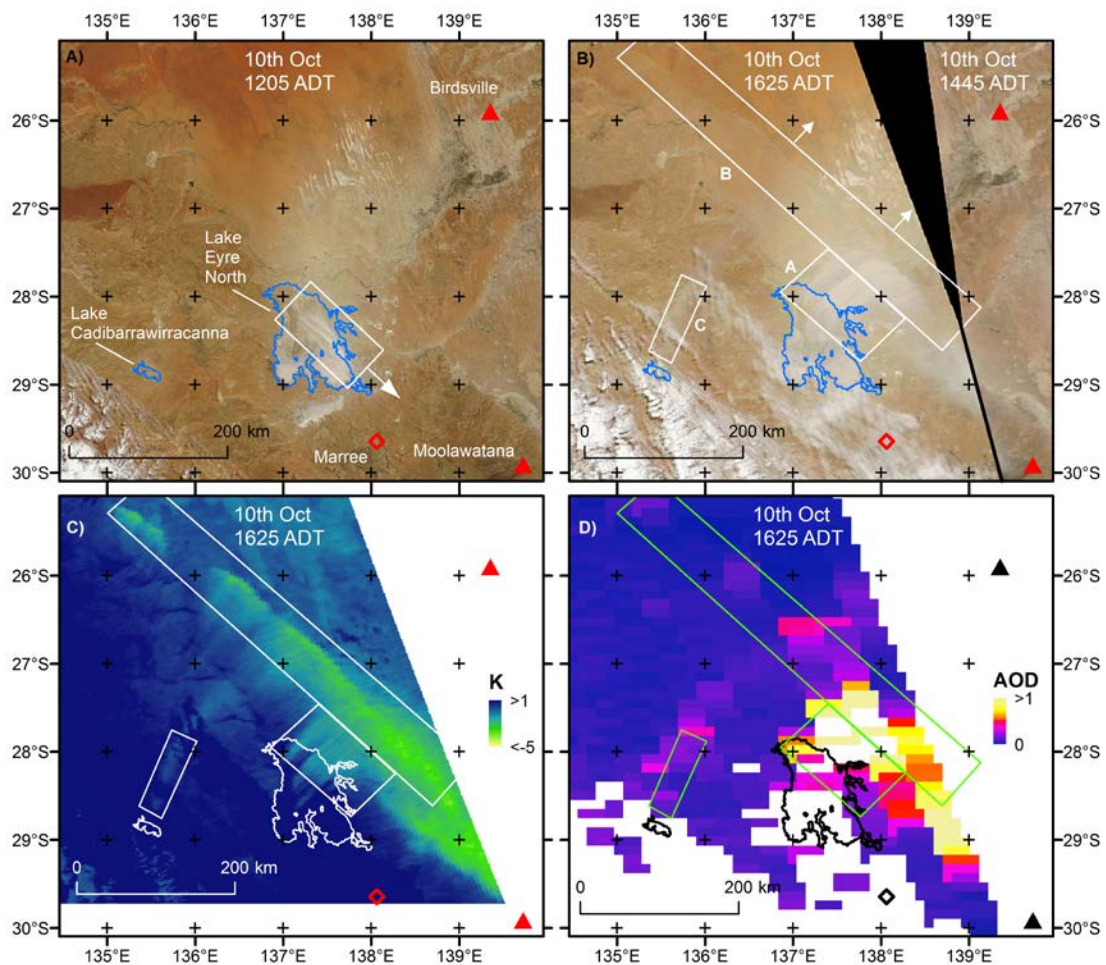
447

448

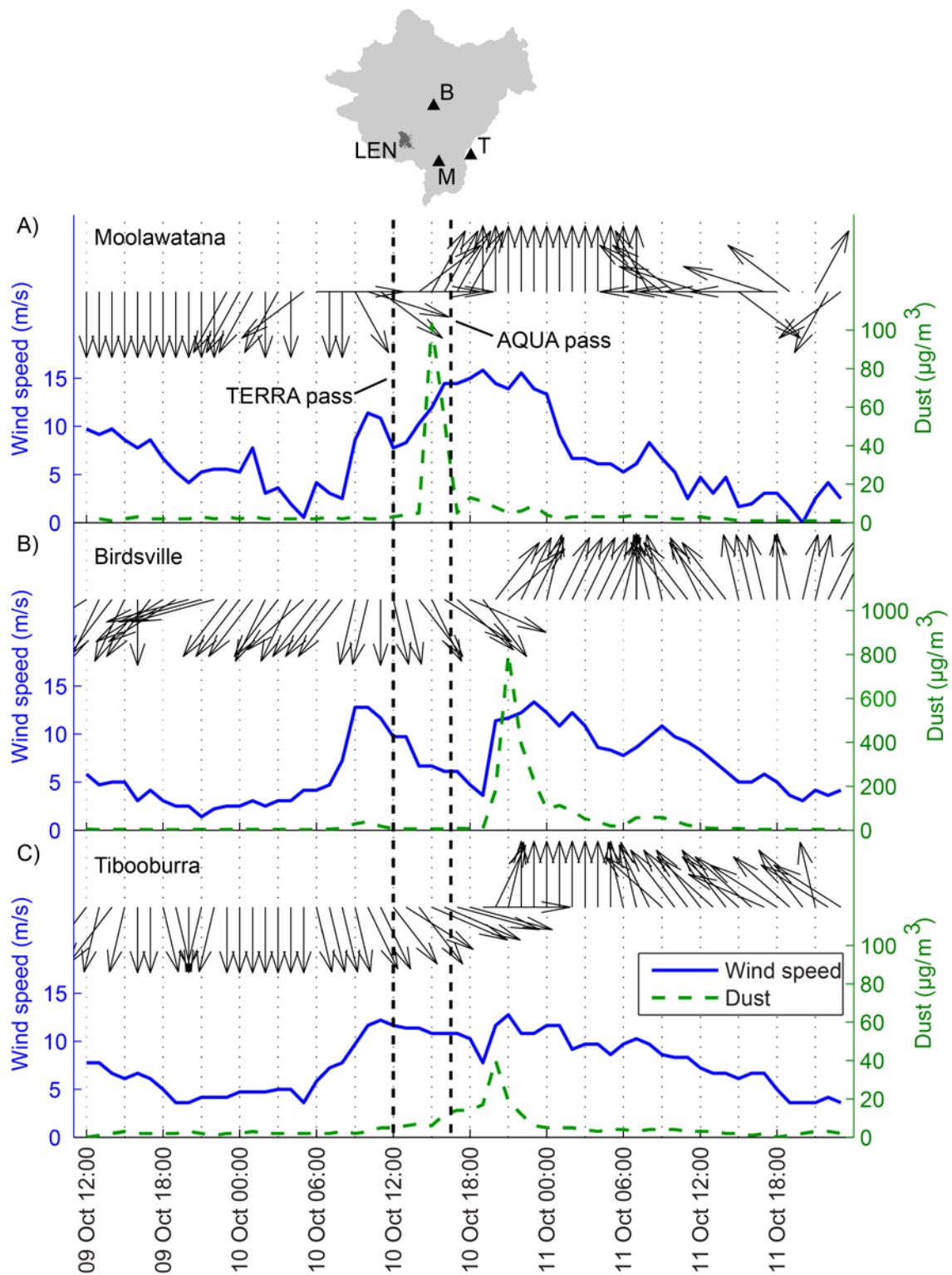
449

450

Figure 3: Mean sea level pressure charts for selected times before, during and after the lower Lake Eyre Basin dust event occurring on the 10th October 2013. (Re-drawn from the Australian Bureau of Meteorology.)



451
 452 Figure 4: A) Terra MODIS 'true colour' scene for 0105 UTC (1205 EDT) 10th October 2013.
 453 B) Aqua MODIS 'true colour' scenes for 0525 UTC (1625 EDT) and 0345 UTC (1445 EDT)
 454 10th October 2013. See time annotations on scenes. C) Brightness temperature difference
 455 (bands 31 and 32) (BTD) for the 0525 scene. Data scaled to a range known to represent dust
 456 in LEB cases, with dust typically having a negative BTD value (see Baddock et al., 2009). D)
 457 MODIS Deep Blue 550 nm aerosol optical depth (AOD) product for 0525 UTC scene only.
 458 True colour imagery from NASA LANCE Rapid Response facility.



459

460 Figure 5: Wind speed, direction and dust concentration ($\mu\text{g}/\text{m}^3$ of PM_{10}) for the dust event at
 461 three DustWatch sites of A) Moolawatana, B) Birdsville and C) Tibooburra. Contextual map
 462 shows location of sites in relation to primary dust source, Lake Eyre North. Note the much
 463 larger scale for dust concentration at Birdsville, and that meteorological data on the
 464 Moolawatana plot is taken from Marree (See text and Figure 2 for locations). Time of the
 465 marked Aqua pass is the 1625 EDT scene (Figure 4b).